An - Najah Univ. J. Res. (N.Sc.) Vol. 20, 2006

Finite Element Analysis of Hyperbolic Paraboloid Groined Vault Structure

استخدام نظرية العناصر المحددة في حل منشأ على شكل قبو ملتوي

Attia Mousa

Department of Civil Engineering, Faculty of Engineering, Islamic University, Gaza, Palestine

E-Mail: attiamousa@hotmail.com

Received: (7/11/2004), Accepted: (23/5/2006)

Abstract

A new hyperbolic parabolic triangular finite element is developed in this paper. The element has only five essential nodal degrees of freedom (three general external degrees of freedom and two rotations) at each of the three corner nodes. The displacement fields of the element satisfy the exact requirements of rigid body modes of motion. Shallow shell formulation is used and the element is based on an independent strain assumption insofar as it is allowed by the compatibility equations. A hyperbolic Paraboloid shell dam for which a previous solution exists is first analyzed using this new element to validate the program and to compute the results. The element is then used in the analysis of a complex type of hyperbolic Paraboloid shell roof, which normally referred to as hyperbolic Paraboloid groined vault. It is usually made up of a combination of four of intersecting hyper Paraboloids joined together to form a square shape in plan view. This form of structure is often used by architects to roof large span exhibition halls and public buildings. The distribution of various components of forces is obtained to give designers an in–sight of the behavior of such complex structures.

ملخص

تم في هذه الدراسة تطوير واشتقاق معادلات الإزاحة باستخدام طريقة العناصر المحددة لعنصر مثلثي جديد على شكل قطع (Hyper)، يحتوي هذا العنصر على خمس درجات حرية عند كل نقطة طرفية (Nodes)، وهي (حركات الإزاحة الثلاثة الرئيسية بالإضافة إلى حركتي الدوران)، ومعادلات الإزاحة للعنصر تلبي المتطلبات الدقيقة لأنماط الحركة للأجسام الصلبة، في هذا الاشتقاق تم استخدام صيغ المعادلات الخاصة بالقشريات الضحلة العمق (shallow) اعتمد العنصر على استقلالية التشوه ضمن حدود المعادلات الانسجامية. تم استخدام المعادلات المشتقة لحل منشأ هندسي عبارة عن سد (Hyper dam) حيث يوجد حل سابق لهذا المنشأ وذلك للتأكد من دقة معادلات العنصر الجديد المستخدم وكذلك للحصول على نتائج باستخدام العنصر الثلاثي الجديد، بعد ذلك تم توسيع العمل في هذا البحث باستخدام معادلات العنصر الجديد لحل منشأ هندسي معقد على شكل قبو منحني مطلق عليه (H.P groin vault)، وهذا النشأ يتكون من تجميع أربع أشكال هايبر (Hyper) متصلة مع بعضها ولتكون شكل مربع في مسقطها الأفقي. هذا النوع من المنشآت يستخدمها عادة المعماريون لتغطية قاعات المعارض والمباني العامة ذات الأبعاد الواسعة، وقد تم الحصول على نتائج للقوة الداخلية للمنشأ والتي من شأنها أن تعطي المهندسين المصممين من خلالها نظرة حول تصرف وسلوك مثل هذا النوع من المنشآت المعقدة.

Introduction

Considerable attention has been given to applying the finite element method of analysis to curved structures. The early work on the subject was presented by Grafton and Strome [(1)] who developed conical segments for the analysis of shells of revolution. Jones and Strome [(2)] modified the method and used curved meridional elements which were found to lead to considerably better results for the stresses.

Further research led to the development of curved rectangular as well as cylindrical shell elements, Connor and Brebbia [(3)], Bonger et al [(4)],

Cantin and Clough [5], and Sabir and lock [6]. However, to model a shell of arbitrary or triangular shape by the finite element method, a triangular shell element is needed. Thus many authors have been occupied with the development of curved triangular shell elements and consequently many elements of lindberg et al [7] and Dawe [8], resulting in an improvement of the accuracy of the results. However this improvement is achieved at the expense of more computer time as well as storage to assemble the overall structural matrix.

Meanwhile, at United Kingdom, a simple alternative approach has been used to the development of curved elements. This approach is based on determining the exact terms representing all the rigid body modes together with the displacement functions representing the straining of the element by assuming independent strain functions insofar as it is allowed by the compatibility equations. This approach has successfully employed in the development of curved shell elements by Ashwell et al [9-10], and by Sabir et al [11-14], and by Mousa [15-16]. These elements were found to yield faster convergence when compared with other available finite elements.

In reference [17], Mousa used the strain-based approach to develop a curved triangular shallow shell element which is suitable for the analysis of hyperbolic Paraboloid shell Structures. The element processes has six degrees of freedom at each corner node. This element was applied to the analysis of a hyperbolic Paraboloid dam with constant thickness and the dam is assumed to be in a rigid valley.

The strain-based approach is employed in the present paper to develop a new triangular strain-based hyperbolic Paraboloid element having only five degrees of freedom at each corner node.

The new element is first tested by applying it to the analysis of a hyperbolic Paraboloid dam with constant thickness for which a previous solution exists.

The work is then extended to the analysis of a complex type of hyperbolic Paraboloid shell roof, which is normally referred to as hyperbolic Paraboloid groined vault. It is usually made up of a

combination of four hyperbolic Paraboloid shell together to form square shape in the plan view. This form is often used by Architects to provide aesthetically pleasing structures with relatively large unobstructed spans. They have been used for exhibition halls and other public buildings.

The distribution of the various components of stresses is obtained to give designers an insight into the behavior of such complex structures.

Displacement function for the new strain-based hyperbolic Paraboloid triangular shell element

Theoretical considerations

In a system of curvilinear coordinates, the simplified strain-displacement relationship for the hyper shell element shown in Figure (1) can be written as:

$$\varepsilon_x = \frac{\partial u}{\partial x} + \frac{w}{r_x}$$

$$\varepsilon_y = \frac{\partial v}{\partial y} - \frac{w}{r_y}$$

$$\gamma_{xy} = \frac{\partial u}{\partial y} + \frac{\partial v}{\partial x} \qquad (1)$$

$$K_x = \frac{\partial^2 w}{\partial x^2}$$

$$K_y = \frac{\partial^2 w}{\partial y^2}$$

$$K_{xy} = -2\frac{\partial^2 w}{\partial x \partial y}$$

Where u,v and w are the displacement in the x,y and z axes, ε_x , ε_y are the in-plane direct axial and circumferential strains and γ_{xy} is the in-plane shearing strain. Also K_x,K_y and K_{xy} are the mid-surface changes of curvatures and twisting curvature respectively, r_x, and r_y are the principle radii of curvature.

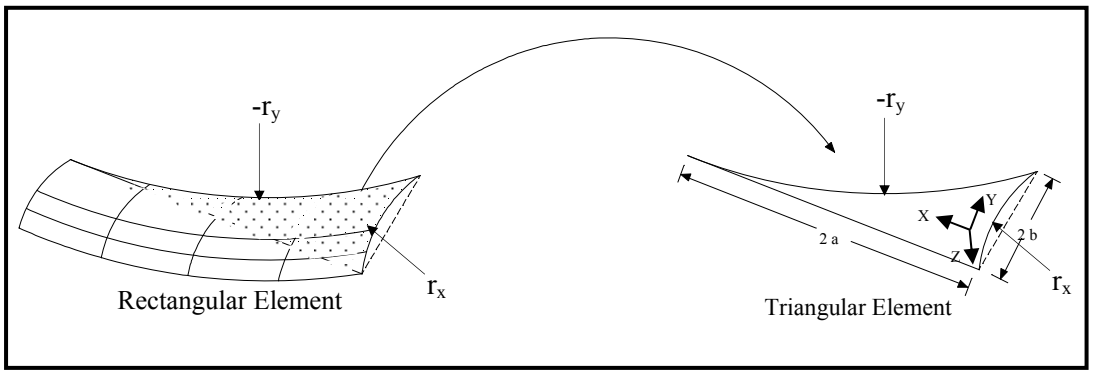

Figure (1): Geometry and co-ordinate axes of triangular hyper shell element.

Equation (1) gives the relationships between the six components of the strain and the three displacements u,v and w. Hence, for such a shell there must exist three compatibility equations which can be obtained by eliminating u,v and w from equation (1).

This is done by a series of differentiations of equation (1) to yield the following compatibility equations:

$$\frac{\partial^2 \varepsilon_x}{\partial y^2} + \frac{\partial^2 \varepsilon_y}{\partial x^2} + \frac{\partial^2 \gamma_{xy}}{\partial x \partial y} - \frac{K_x}{r_y} + \frac{K_y}{r_x} = 0.0$$

$$\frac{\partial K_{xy}}{\partial x} - 2\frac{\partial K_y}{\partial y} = 0 \qquad (2)$$

$$\frac{\partial K_{xy}}{\partial y} - 2\frac{\partial K_x}{\partial x} = 0$$

To keep the triangular element as simple as possible, and to avoid the difficulties associated with internal and non-geometric degrees of freedom, the essential five degrees of freedom at each corner node are used, namely u, v,w, $\partial w/\partial x, \partial w/\partial y$. Thus, the triangular hyper element, to be developed has a total of fifteen degrees of freedom and 15x15 stiffness matrix.

To obtain the rigid body components of the displacement field, all the strains, as given by equations (1), are set to zero and the resulting partial differential equations are integrated. The resulting equations for u, v and w are given by:

$$u_1 = -a_1 x/r_x - a_2 (y^2/2r_y + x^2/2r_x) - a_3 xy/r_x + a_4 + a_6 y$$
$$v_1 = +a_1 y/r_y + a_2 xy/r_y + a_3 (+y^2/2r_y - x^2/2r_x) + a_5 - a_6 x \quad (3)$$
$$w_1 = a_1 + a_2 x + a_3 y$$

Where u_1, v_1 and w_1 are the rigid body components of the displacement fields u, v and w, respectively, and are expressed in terms of the six independent constants a_1, a_2 … a_6.

Since the element has fifteen degrees of freedom, the final displacement fields should be in terms of fifteen constants. Having used six for the representation of the rigid body modes, the remaining nine constants are available for expressing the straining deformation of the element. These nine constants can be apportioned among the strains in several ways, for the present element we take:

$$\varepsilon_x = a_7 - \frac{1}{r_x}(a_{12} y^{2}/_{2} + a_{13} xy^{2}/_{2} + a_{14} y^{3}/_{6})$$

$$\varepsilon_y = a_8 + \frac{1}{r_y}(a_{10} x^{2}/_{2} + a_{11} yx^{3}/_{6}) \quad (4)$$

$$\gamma_{xy} = a_9$$

$$K_x = a_{10} + a_{11} xy$$

$$K_y = a_{12} + a_{13} x + a_{14} y$$

$$K_{xy} = a_{15} + [a_{11} x^2 + 2a_{13} y]$$

In which the unbracketed independent constants terms in the above equations were first assumed. The linking bracketed terms are then added to satisfy the compatibility equation (2).

Equations (4) are then equated to the corresponding expressions, in terms of u,v and w from equations (1) and the resulting equations are integrated to obtain:

$u_2= a_7x + a_9y/2 + a_{10}x^3/6r_x + a_{11}x^4y/24r_x + a_{13}y^4/24r_y + a_{15}\ (x^2y/4r_x + y^3/12r_y)$.

$v_2= a_8y + a_9x/2 - a_{11}x^5/120r_x - a_{12}y^3/6r_y - a_{13}xy^3/6r_y - a_{14}y^4/24r_y - a_{15}\ (xy^2/4r_y + x^3/12r_x)$.

$w_2= - a_{10}\ x^2/2 - a_{11}x^3y/6 - a_{12}\ y^2/2 - a_{13}xy^2/2 - a_{14}y^3/6 - a_{15}xy/2$ (5)

The complete displacement functions for the element are the sum of corresponding expressions in equations (3) and (5). The rotation about the x and y-axes respectively, are given by:

$$\varphi y = -\frac{\partial w}{\partial x} = -a_2 + a_{10}x + a_{11}x^2y/2 + a_{13}y^2/2 + a_{15}y/2$$
$$\varphi x = -\frac{\partial w}{\partial y} = -a_3 + a_{11}x^3/6 - a_{12}y - a_{13}xy - a_{14}y^2/2 - a_{15}x/2 \quad (6)$$

The stiffness matrix [K] for the shell element is calculated in the usual manner using the equation.

$$K = \left[C^{-1}\right]^T \left\{\iiint B^T DBdv\right\}\left[C^{-1}\right] \quad (7)$$

Where B and D are the strain and rigidity matrices respectively and C the matrix relating the no dal displacements to the constants a_1 to a_{15},B can be calculated from equations (1), (3) and (5) and D is given below.

Substituting the matrices B and D into equation (5), the integrated within the bracketed terms of equation (4) are carried out explicitly and the rest of the calculations are computed to obtain the stiffness matrix [K]

$$[D]=\frac{Et}{1-v}\begin{bmatrix} 1 & v & 0 & 0 & 0 \\ v & 1 & 0 & 0 & 0 \\ 0 & 0 & \frac{1-v}{2} & 0 & 0 \\ 0 & 0 & 0 & \frac{t^2}{12} & \frac{vt^2}{12} \\ 0 & 0 & 0 & \frac{vt^2}{2} & \frac{t^2}{2} \end{bmatrix}$$

Where E is Young's modulus, t is the thickness and *v* is Poisson's ratio.

Consistent load vector

In the finite element analysis, if the structure is subjected to any of distributed vertical loading q, the equivalent set of nodal forces must be first calculated, the simplest way is to allocate specific areas as contributing to a node, such process is known as the lumping process. An alternative and more accurate approach for dealing with distributed load is the use of the consistent load vector. This is obtained by equating the work done by applied distributed load on the displacement of the element to the work done by nodal generalized forces on the nodal displacements. If a triangular shell element is subjected to distributed load of intensity q per unit area in the direction of w, the work done by this load F_1 is given by:

$$F_1 = \int_{-b}^{b}\int_{ay/b}^{a} qwdxdy \qquad (9)$$

Where a and b are the projected half-length of the sides of a right angle triangular element in the x and y directions, respectively. If w is taken to be represented by:

$$\{w\} = [N^T]\{a\}=[N^T][C^{-1}]\{d\} \qquad (10)$$

Where N^T for the present element is given by [see equations (3) and (5))

$N^T = [1,x, y, 0,0,0,0,0,0,-x^2/2, -x^3y/6, -y^2/2, -xy^2/2, -y^3/6, -xy/2]$ (11)

{a} is a vector of the independent constants, $[C^{-1}]$ is the inverse of the transformation matrix and {d} is a vector of the nodal degrees of freedom, the work F_2 done by the consistent nodal generalized forces {p} on the nodal displacement {d} is given by"

$$F_2 = \{p\}^T\{d\}$$

Hence from eqs (9), (10) and (11) we obtain:

$$\{p\} = \int_{-b}^{b}\int_{ay/b}^{a} q[N]^T[C]^T\{d\} = [N]^{-1}\,dxdy \qquad (12)$$

The above equation gives the nodal forces for a single element and these are then used in calculating the nodal forces for the whole structure. This is achieved by adding the contributions from all the elements meeting at each node.

Problems considered

Hyperbolic Paraboloid dam

The accuracy of the finite element results obtained from the use of the strain- based triangular element developed in the present Paper is demonstrated by applying it to hyperbolic Paraboloid shell dam.

The problem considered is that of hyperbolic dam shown in Figure (2). The dam has the following dimensions and elastic properties:

$r_x = -r_y = 43.25$m, thickness (t)= 3m, height (h)= 30m, $\nu = 0.16$, and E= 210×10 kn/m2, it is subjected to Hydrostatic Pressure. The dam is assumed to be in a rigid valley and the external boundaries of the dam are assumed to be fixed for all the degrees of freedom at each nodal points.

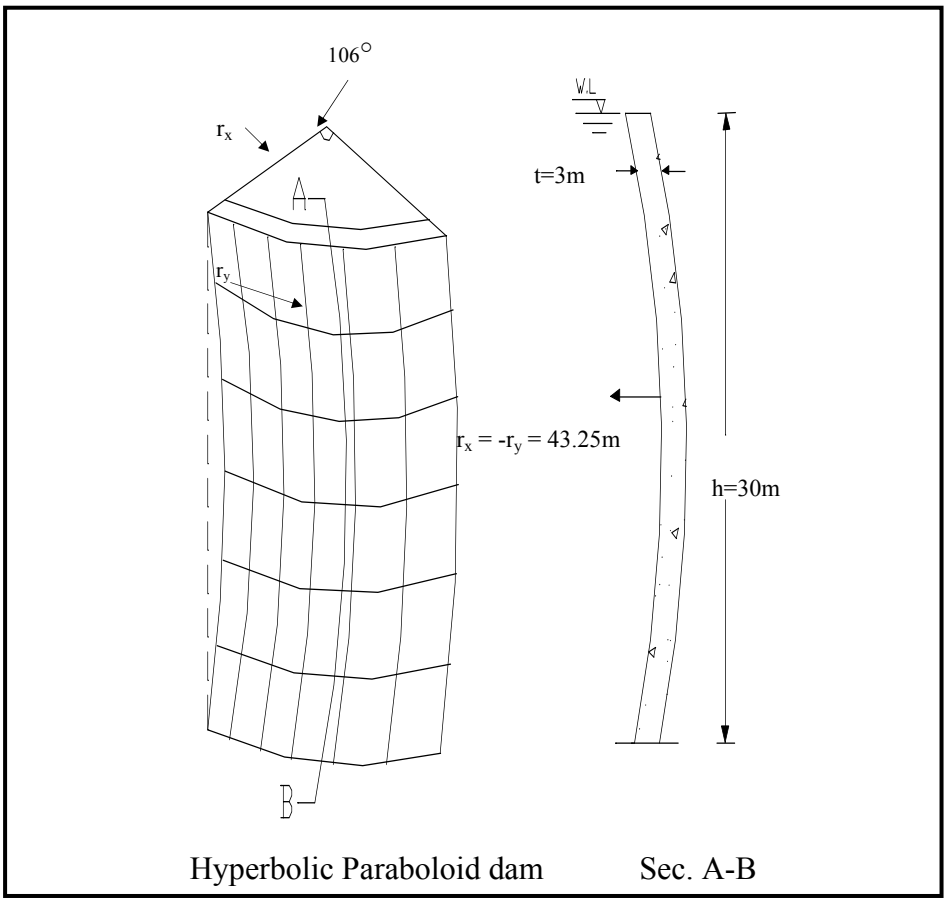

Figure (2): General Dimensions of Hyperbolic Paraboloid Dam.

This problem was analyzed previously by Mousa [17] using a triangular hyper element with six degrees of freedom at each corner node. Now the new strain based triangular hyper element developed in the present paper is applied to analyze the same problem, the mesh considered in the previous element (207 triangular elements) is shown in Figure (3).

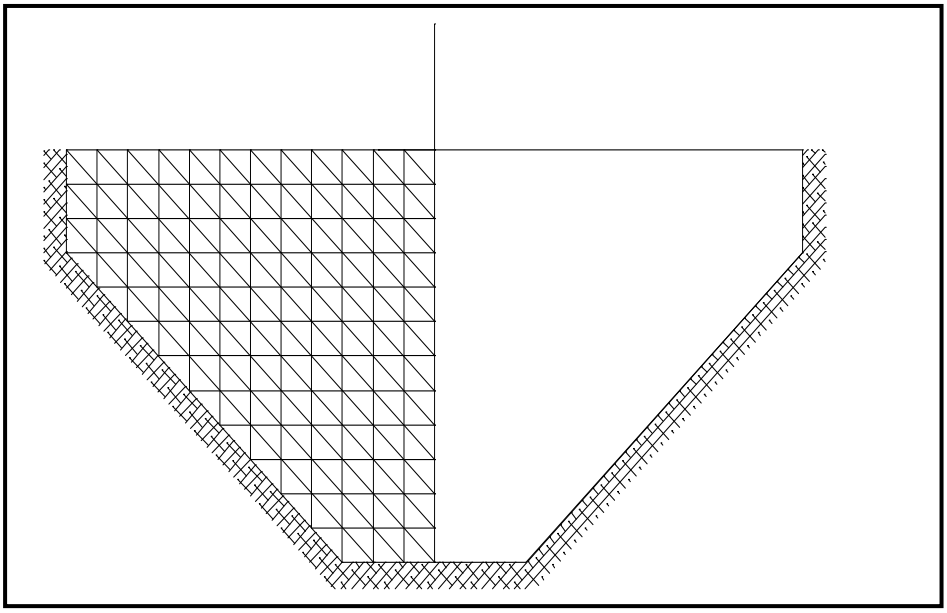

Figure (3): Finite element mesh in the H.P. dam.

The results for the normal deflection along the vertical central line using the same mesh size are given in Figure (4). Figures (5) to (8) give the results for the vertical stresses and hoop stresses on both the upstream and down stream faces, respectively, using the same mesh size.
The figures show that the present element gives a very good agreement results.

It is found that the shell needs to be modeled by few elements to obtain a very good agreement results for the deflection and stresses, these results gave confidence in applying the present triangular hyper element to the practical and complex problem of a hyper shell roof such as hyperbolic parabolic groined vault.

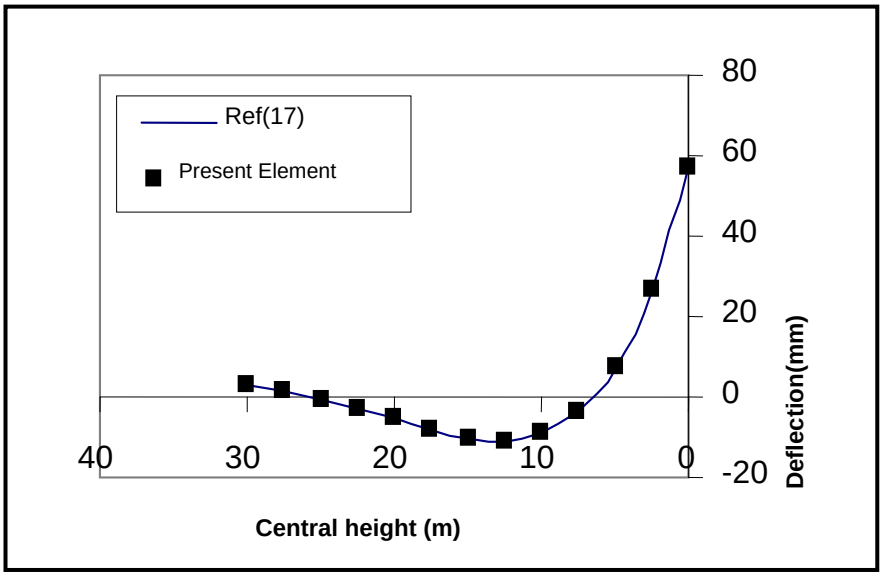

Figure (4): Radial deflection on central line of dam

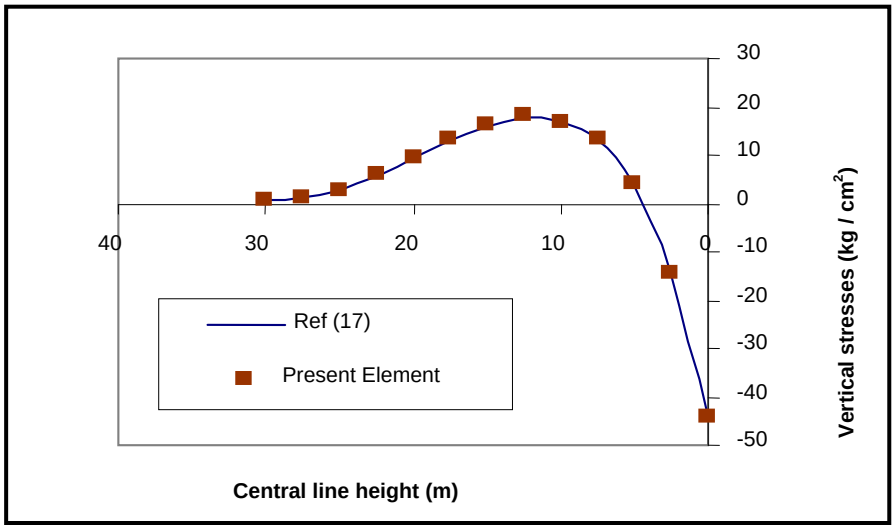

Figure (5): Vertical Stresses on central cantilever for dam (upstream)

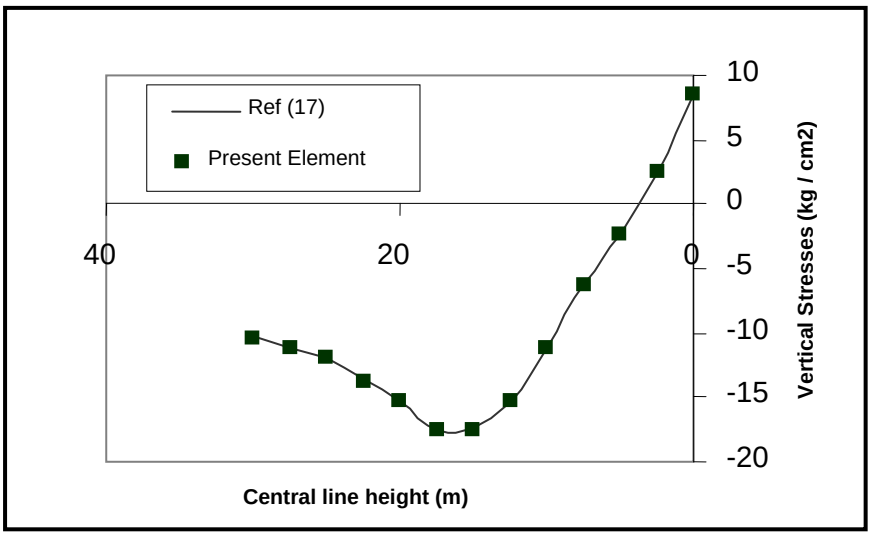

Figure (6): Vertical stresses on central of dam (down stream).

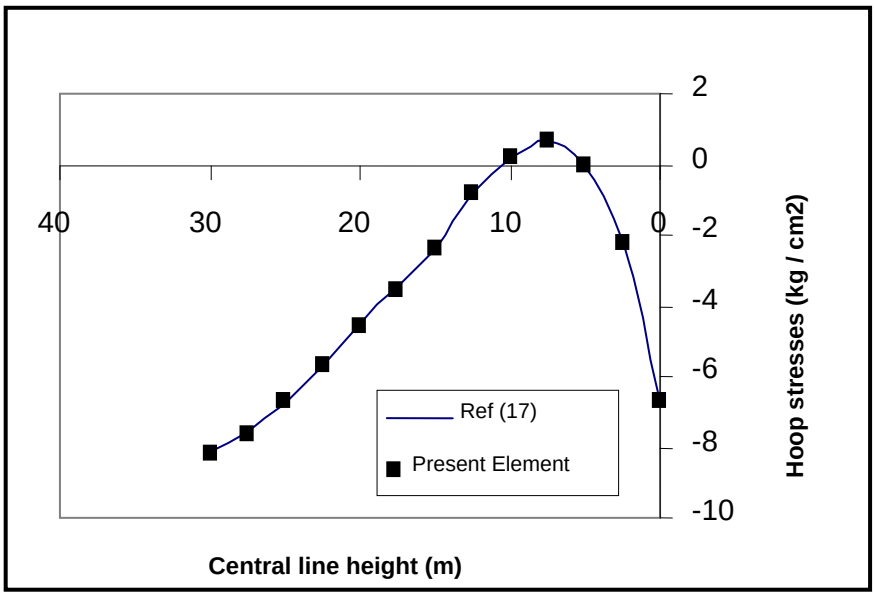

Figure (7): Hoop stresses on central cantilever of dam (upstream).

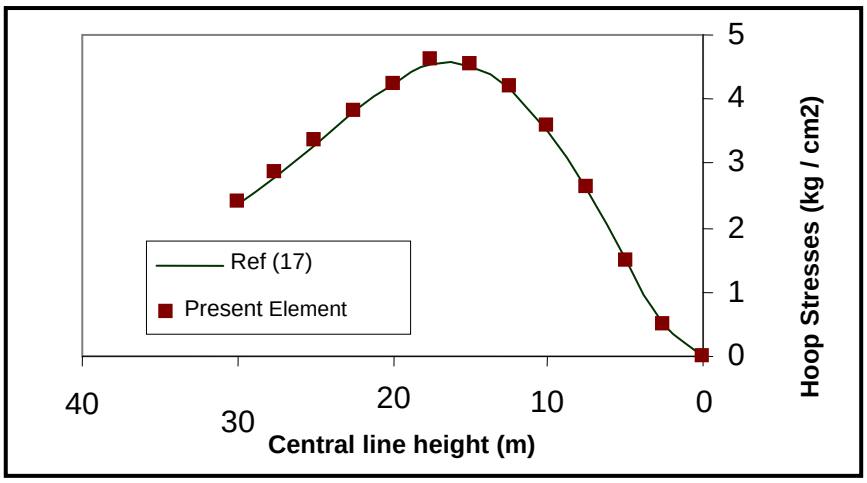

Figure (8): Hoop stresses on central cantilever of dam (downstream)

Analysis of hyperbolic paraboloid groined vault:

The complex type of a hyperbolic paraboloid shell roof, which is usually referred to as the hyperbolic paraboloid groined vault is analyzed in this section.

The structure consists of four intersecting hyper joints together to form a square shape in the plan view, as shown in Figure (9).

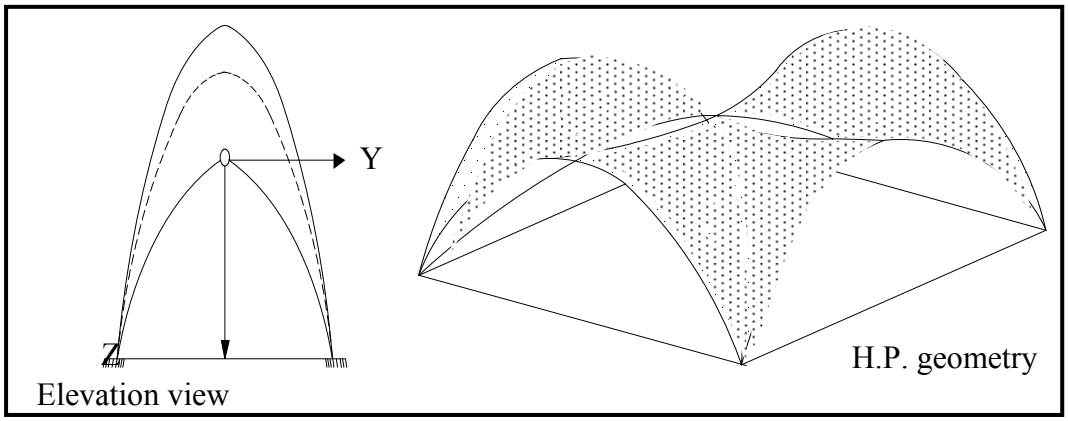

Figure (9): Hyperbolic paraboloid groin vault roof.

The model investigated is shown in Figure (10), the shell roof is supported on its four low corners, the interior boundaries of the shell are jointed in the groin arch spanning between support points. The exterior edges of the shell are kept free and the groined arch consists of a V cross section

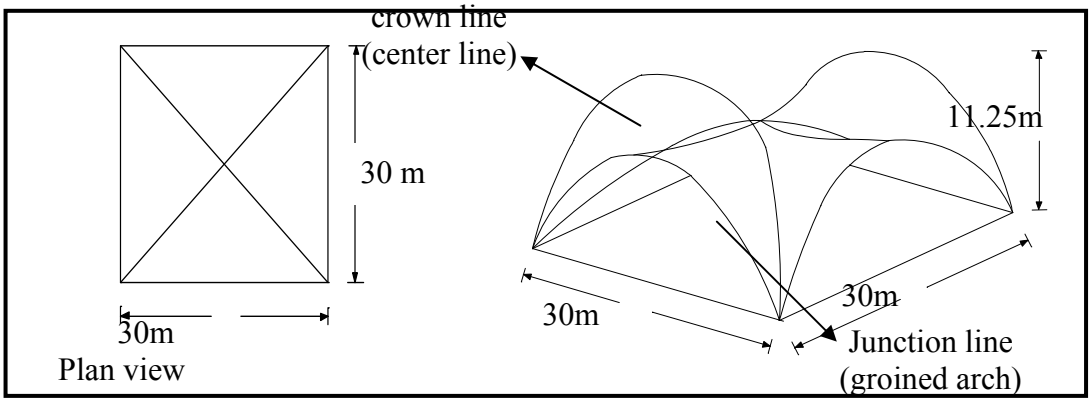

Figure (10): Groined vault roof dimensions and configuration.

As shown in Figure (10), a hyper-groined vault with straight edges, 30 m by 30 m square in plane is considered; the concrete shell thickness is 10 cm. The dead load of shell plus it's roofing is 0.3N/cm^2 of shell surface and the live load is 0.15N/cm^2 of horizontal projection. The input geometry for a typical segment as shown in Figures (10) and (11), is; A=15m; B=15m, C=11.25 m.

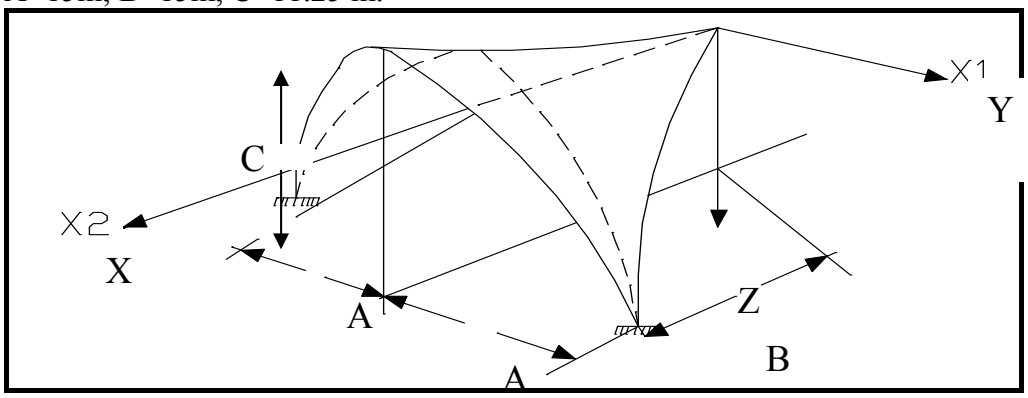

Figure (11): Typical segment of hyperbolic paraboloid roof.

This structure is identical to that one analyzed in Ref [18], using approximate method in which only was analyzed only under the dead load of the shell and the results are obtained only for the axial forces (N_x, N_y) along the central line of the shell.

In the present paper, the developed strain-based triangular hyper element is used in analysis of the same structure and under the dead load only and also analyzed under dead load and live load together.

Due to Symmetry and uniform loading, only one quadrant of the shell is analyzed. The conditions for symmetry along the straight edges are taken to be:

(a) Along the centerline (crown line) of the segment, the circumferential displacement and rotation about the central line are zero.

(b) Along the junction arch, because of symmetry, the horizontal displacement and rotation about the junction arch are zero. These conditions, however, cannot be satisfied directly, due to discontinuity of the slope of the middle surface of the shell along the junction (see Figure (12)). This difficulty is overcame by transferring the co-ordinates of the nodes of all elements adjacent to the line of symmetry into a common set of co-ordinate axes.

Details of such transformations are given by Mousa and Sabir [15].

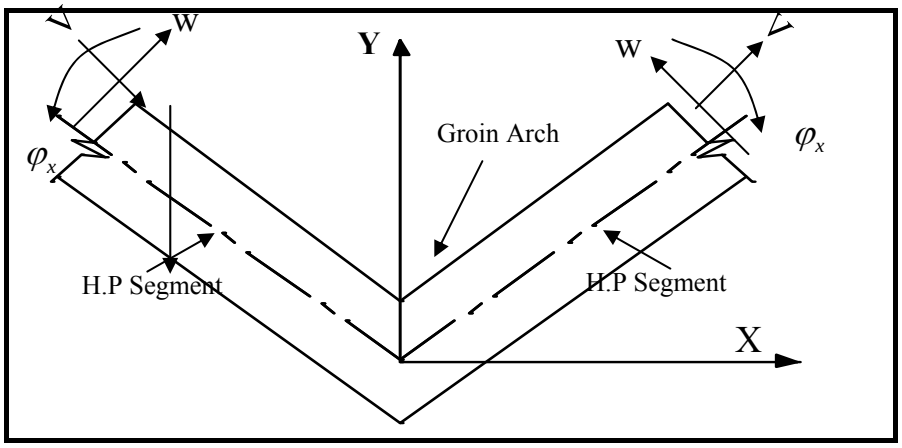

Figure (12): Displacement transformation at the joint of the two segment.

Due to symmetry only one half of the segment shell is analyzed. The mesh shown in Figure (13) is considered.

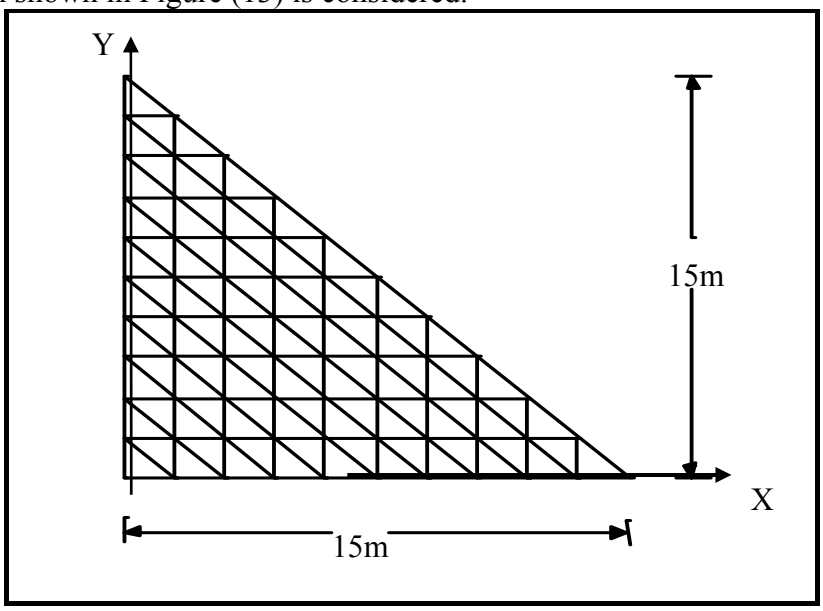

Figure (13): Finite element mesh.

The results for the N_x and N_y stresses (under dead load only, 0.15N/cm) at the center line (crown line) are given in Figures (14) and (15), respectively. These figures show the results obtained by the new element and those plotted in reference [18].

The figures show that the present element gives a good agreement results.

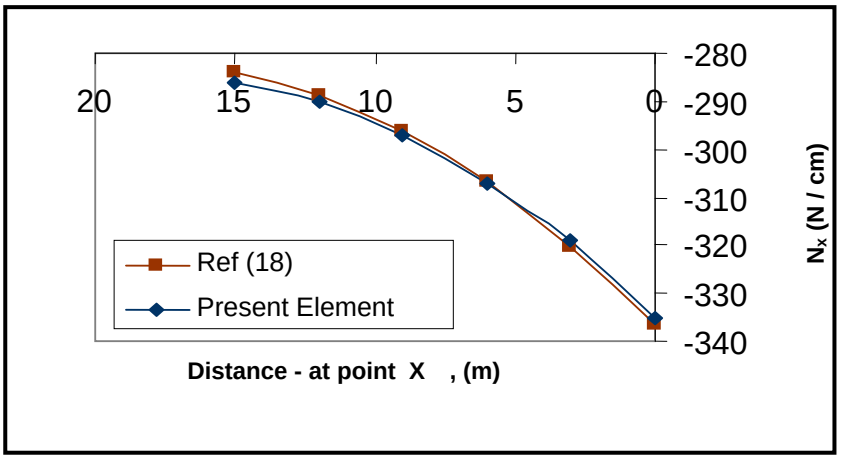

Figure (14): Axial force (N_X) along the central line of shell.

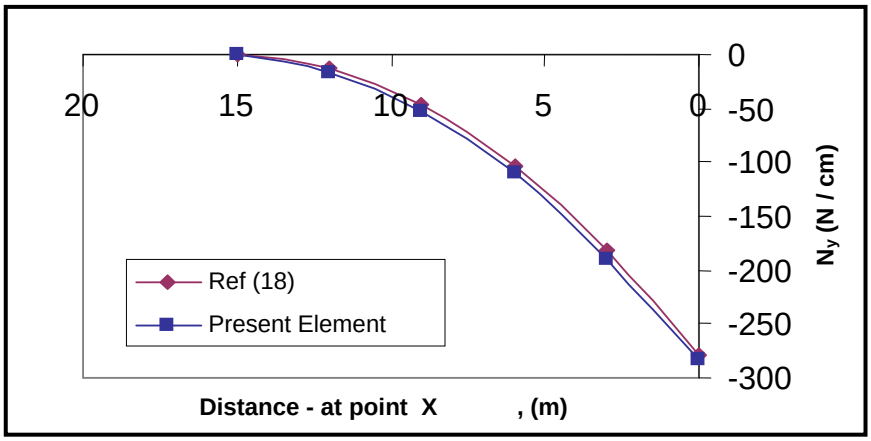

Figure (15): Axial force N_y along the central line of shell.

The results for the normal force, shear force and bending moment (under dead and live loads together, 0.30N/cm, 0.15N/cm) along the groined arch, (Junction line), they are also obtained and given in the Figures (16-17) and Figure (18) respectively.

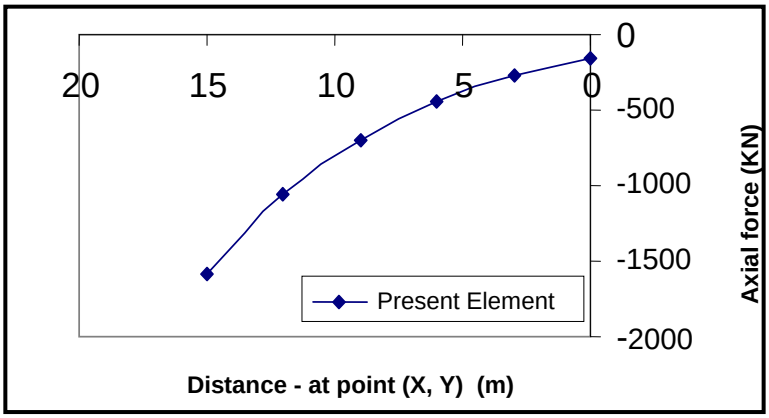

Figure (16): Internal axial force along the groin arch.

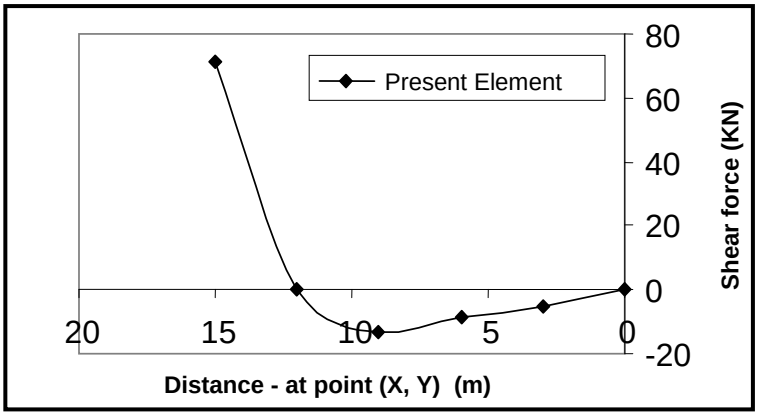

Figure (17): Internal shear force along the groin arch.

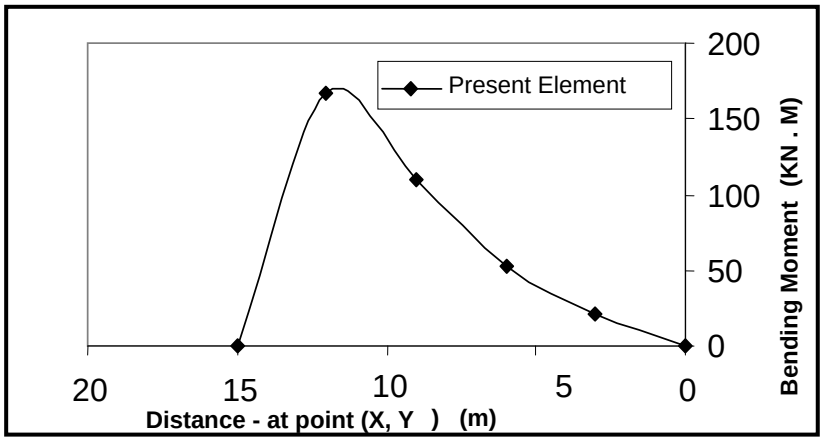

Figure (18): Internal bending moment (M_x) along the groin arch.

To study the effect of curved overhanging free edges of the shell structures, two additional groined vaults, having the basic dimensions of the preceding example are analyzed using the previous dead and live loads. The three additional structures have curved overhangs, parabolic in the plan view, with 3m, 6m maximum projections, as shown in Figure (19).

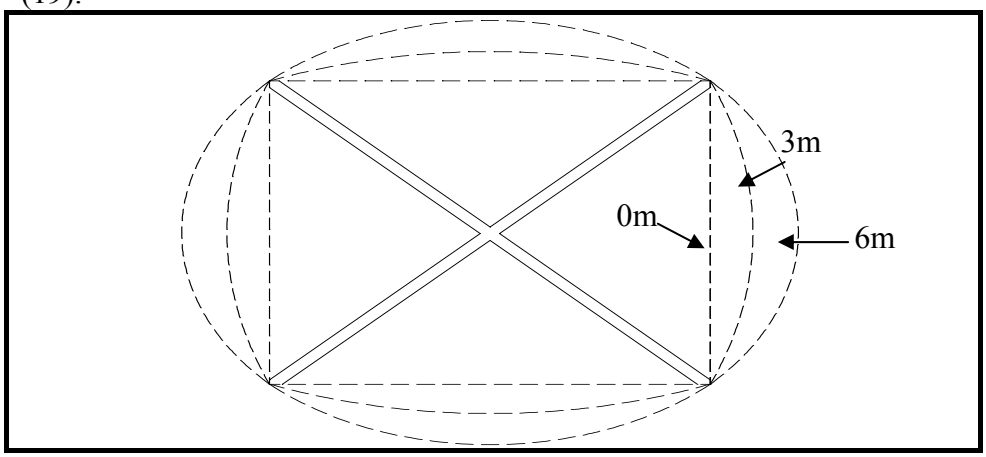

Figure (19): Plan view of structure with various free edge overhanging projections.

A comparison of the internal forces (normal force, shearing force and bending moment) along the groined arch (Junction line) for the 0,3, and 6m projection cases are given in Figures (20, 21) and Figure 22.

It can be seen from the Figures (20 to 22) that there is a significantly greater change in the bending moment than the axial force as the overhang increase from 0 to 6m.

There is also a slight shift of the point of maximum moment towards the support.

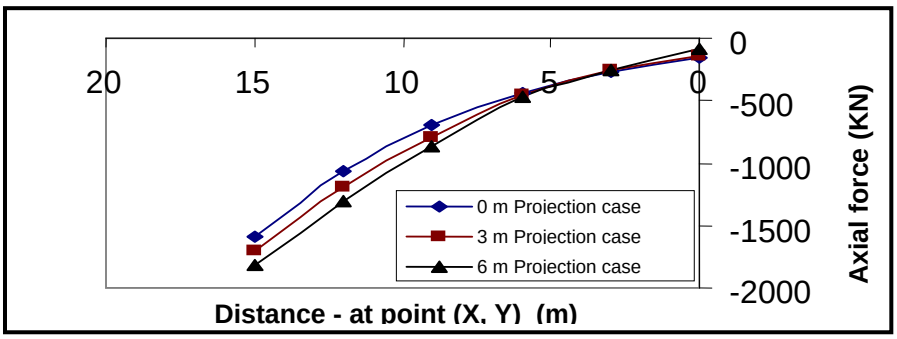

Figure (20): The effect of overhanging on the internal axial force along the groin arch.

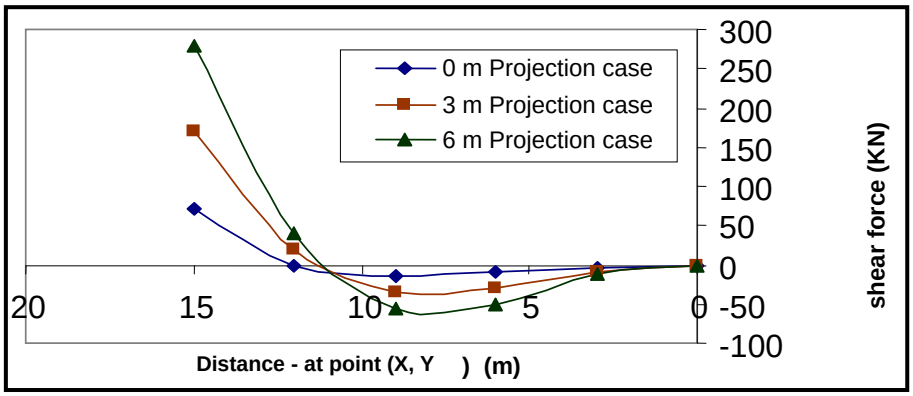

Figure (21): The effect of overhanging on the central shear force along the groin arch.

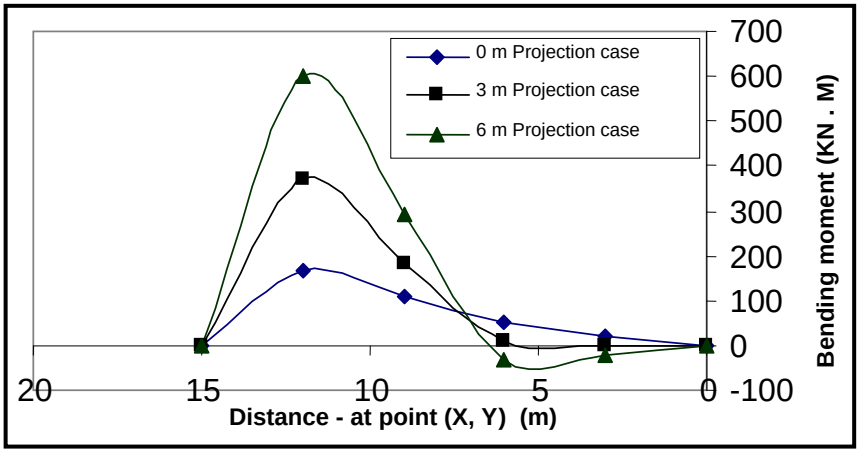

Figure (22): The effect of overhanging on internal bending moment along the groin arch.

Conclusions

A new triangular strain-based finite hyperbolic paraboloid element is developed using shallow shell formulation. The element has the essential five degrees of freedom at each corner node.

The developed triangular hyper finite element is first applied to analysis of a hyperbolic Paraboloid dam. The results for the deflections and stresses are presented, and show that the developed element gave a very good agreement results. This element is then used to analyze a hyperbolic Paraboloid groined vault and the various components of internal forces are given.

The effect of a curved overhanging free edge of the groined vaults on the various internal stresses along the groined arch shell are studied, and the various internal forces along the groin arch are presented.

It is found that there is a significantly greater change in the bending moments than in the axial forces as the overhang increases from 0 to 6 m. There is also a slight shift of the point of maximum moment to wards the support.

References

(1) Grafton P.E. and Strome. D.R., "analysis of axisymmetric shells by the direct stiffness method" *AIAA. J.* **1,** (1963), 2342-2347.

(2) Jones. RE and Strome. D.R. "Direct stiffness method analysis of shells of revolution utilising curved dements", *AIAA. J.,* **(4),** (1966), 1519-1525.

(3) Conner. J.J. and Brcbbia, C. "Stiffness matrix for shallow rectangular shell element". *J. Eng. Mech. Div. ASCE,* **93.** No EMS, (1967), 41-65.

(4) Bogncr. F K. Fox. R L. and Schmit. I. A. "A cylindrical shell discrete element", *J. AIAA.,* **5(4),** (1967), 745-750.

(5) Cantin. G and Clough. R.W. "A curved cylindrical shell finite element" *AIAA J.* **16,** (1968), 1057-1062.

(6) Sabir. A.B. and Lock A.C. "A curved cylindrical shell finite element" *Int. J. Mech. Sci*. **14,** (1972), 125-135.,

(7) Lindbergy. G.M. Cowper. G. R. and Olson. M.D. "A shallow shall finite element" ***of triangular shape****" Int. J. Solids struc.* **14,** (1970), 1133-1156.

(8) Dawe. D.J. "High order triangular finite element for shell and analysis" *Int. J. Solids struct.* **11,** (1975), 1097-1110.

(9) Ashwell. D.G. Sabir. A.B. and Roberts T.M. "Further studies in the application of curved finite element to circular studies" *Int. J. Mech. Sci.* **13.** (1971), 507-517.

(10) Ashwell. D.G. and Sabir. A.B, "A new cvlindrical shell finite dement based on simple independent strain functions". *Int. J. Mech. Sci.* **14,** (1972), 171-183.

(11) Sabir A B. "Stif'fness matrices for general deformation (out of plane and in-plane) of curved beam members based on independent strain functions", *The Maths of Finite Elements and Applications II. Academic Press.* **34,** (1975), 411-421.

(12) Sabir A B. and charchafchi. T.A. "curved rectangular and general quadrilateral shell element for cylindrical shells" *The math of Finite Elements and Applications IV. Academic Press* (1982), 231-238.

(13) Sabir. A.B. "Strain based finite for the analysis of cylinders with holes and normally intersecting cylinders". *Nuclear Eng. and Design,* **76,** (1983), 111-120.

(14) Sabir. A.B. "Strain based Shallow spherical shell element" *Proceedings Int. Conf. on the Mathematics of Finite Element and Applications,* Bronel University (1987).

(15) Mousa. A. I. and Sabir. A.B "Finite Element analysis of fluted conical shell roof structures". *Computational structural engineering in practice. Civil Comp. Press,* ISBN 0-948748-30-X pp173-181 (1994).

(16) Mousa A.I "Finite Element analysis of a Gable shell roof" *Advances in Civil and Structural of Engineering Computing for Paretic civil- comp press,* (1998), 26-268.

(17) Mousa. A.I "Finite Element Analysis of shell structures" *UWCC,* Internal Publication, University of Wales, U.k, (1991).

(18) "Elementary Analysis of Hyperbolic Paraboloid shells", *Portland* (Cement Association Bulletin ST 35 (Skoki, Illionis,) (1960).